

Electronic Supplementary Information (ESI)

Optimization of gold-palladium core-shell NWs towards H₂O₂ reduction by adjusting shell thickness

Yongdi Dong,^a Qiaoli Chen, ^{*a,b} Xiqing Cheng,^a Huiqi Li,^a Jiayu Chen,^a Xibo Zhang,^a
Qin Kuang,^{*a} Zhaoxiong Xie^a

^a State Key Laboratory of Physical Chemistry of Solid Surfaces, Collaborative Innovation Center of Chemistry for Energy Materials, Department of Chemistry, College of Chemistry and Chemical Engineering, Xiamen University, Xiamen, 361005, P.R. China.

^b College of Chemical Engineering and State Key Laboratory Breeding Base of Green Chemistry Synthesis Technology, Zhejiang University of Technology, Hangzhou, 310014, China

E-mail: qkuang@xmu.edu.cn; qlchen@zjut.edu.cn

List of contents

Fig. S1	TEM images of Au ₇₅ Pd ₂₅ NWs	S3
Fig. S2	EDX spectra of Au-Pd NWs with different Au/Pd molar ratio	S3
Fig. S3	XPS spectra Au-Pd NWs with different Au/Pd molar ratio	S4
Fig. S4	SEM images of products synthesized with controlling Au/Pd feeding ratio	S4
Fig. S5	Cross-sectional compositional line profiles of Au-Pd NWs with different Au/Pd molar ratio.	S4
Fig. S6	SEM images of products synthesized at different temperatures	S5
Fig. S7	SEM image of the products synthesized with OTAB.	S5
Fig. S8	LSV curves and calibration curves of H ₂ O ₂ electro-reduction for Au and Au-Pd NWs with different Au/Pd molar ratio	S5
Fig. S9	CV curves of Au polycrystalline electrode, Au-Pd nanowires with different Au/Pd ratios and Pd black	S6
Table S1	Comparison of the H ₂ O ₂ sensing performance in this work with that of other Au-Pd nanomaterials.	S6

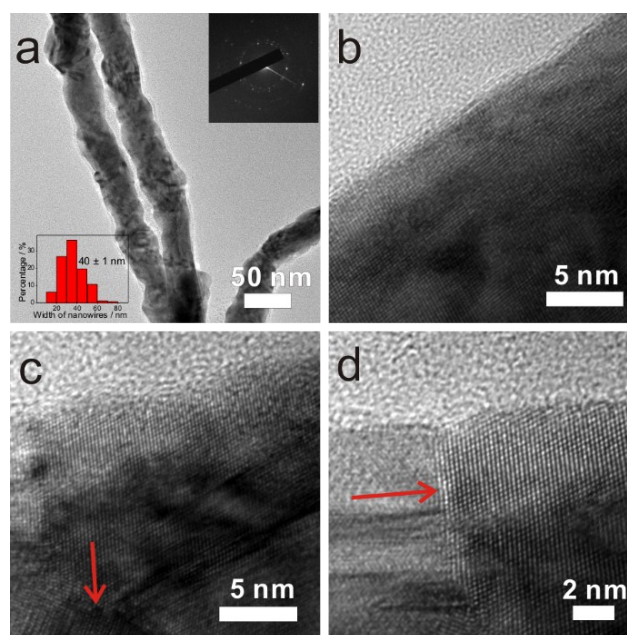


Figure S1. (a) TEM image of Au₇₅Pd₂₅ NWs. The top right inset is the corresponding selected area electron diffraction (SAED) pattern and the bottom left inset is the size distribution histogram of nanowires' width. HRTEM images showing the area of (b) single crystalline, (c) twin boundary and (d) stacking fault in a nanowire.

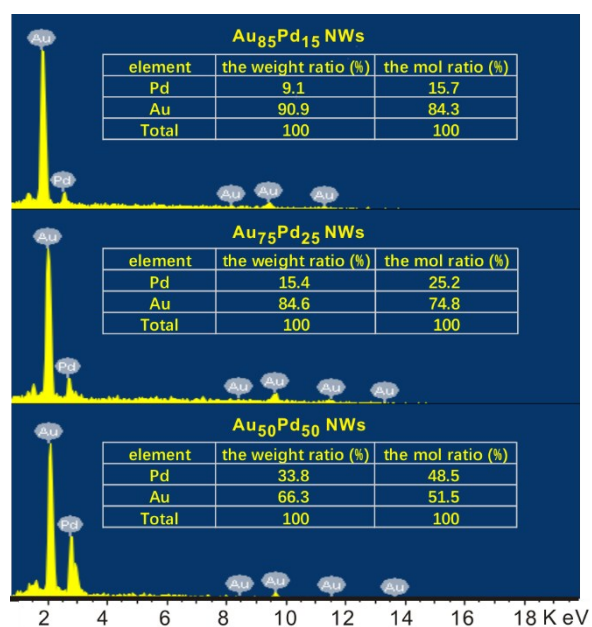


Figure S2. EDX spectra and their corresponding elements contents of Au-Pd nanowires with different Au/Pd ratios.

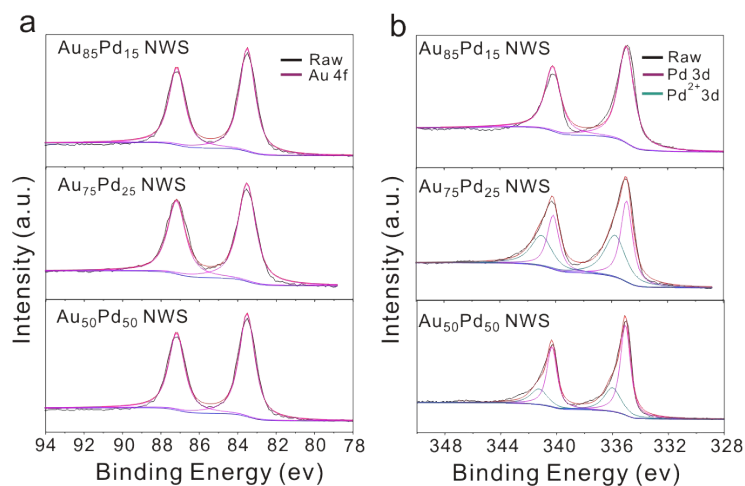


Figure S3. (a) Au 4f and (b) Pd 3d XPS spectra of Au-Pd nanowires with different Au/Pd ratios.

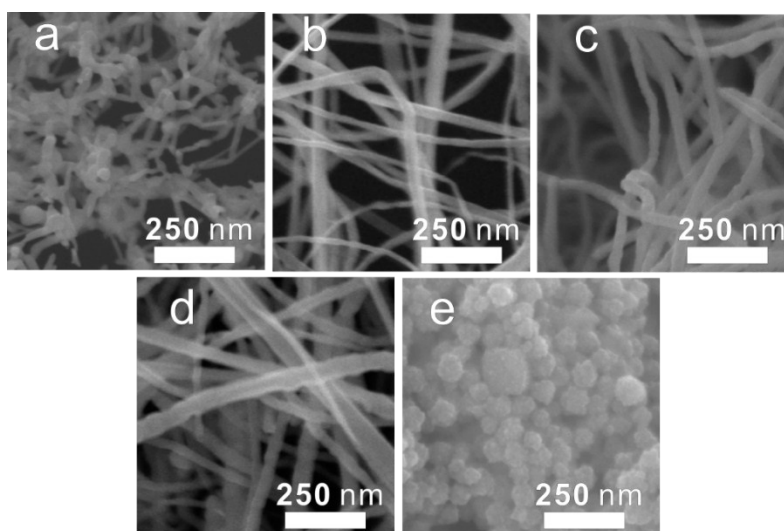


Figure S4. SEM images of the as-synthesised products formed by controlling Au/Pd feeding ratio: (a) Au NWS, (b) Au₈₅Pd₁₅ NWS, (c) Au₇₅Pd₂₅ NWS, (d) Au₅₀Pd₅₀ NWS, (e) Pd NPs.

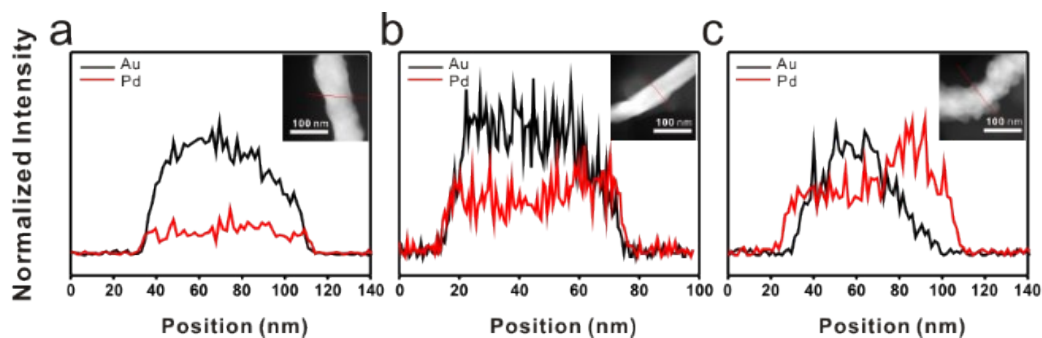


Figure S5. Cross-sectional compositional line profiles of (a) Au₈₅Pd₁₅ NWS, (b) Au₇₅Pd₂₅ NWS, (c) Au₅₀Pd₅₀ NWS.

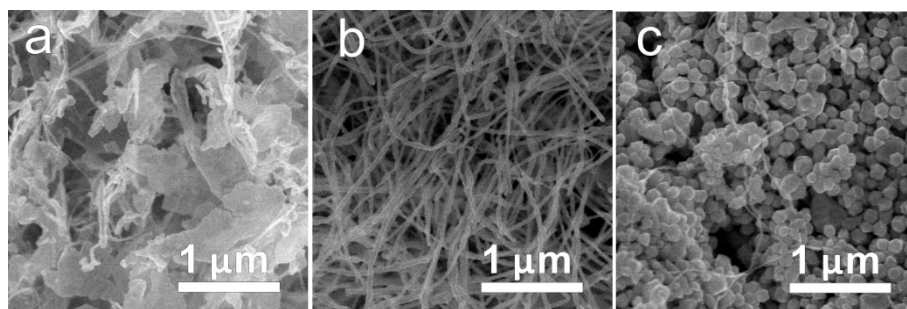


Figure S6. SEM images of products synthesized at different temperatures: (a) 6 °C, (b) 30 °C, (c) 50 °C.

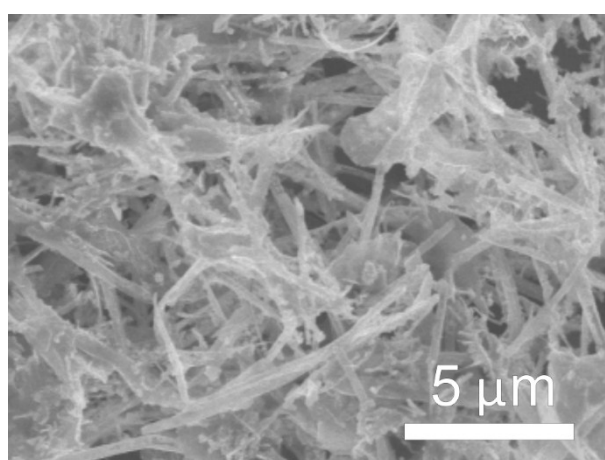


Figure S7. SEM image of the product synthesized with OTAB.

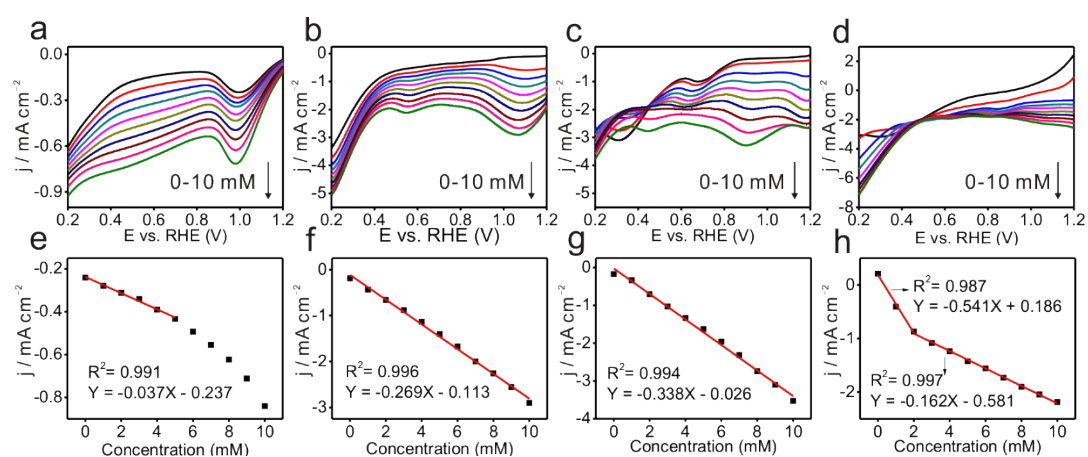


Figure S8. (a-d) LSV curves of H₂O₂ reduction and (e-h) their corresponding H₂O₂ calibration curves at 0.97 V for Au NWs, Au₈₅Pd₁₅ NWs, Au₇₅Pd₂₅ NWs, Au₅₀Pd₅₀ NWs, respectively.

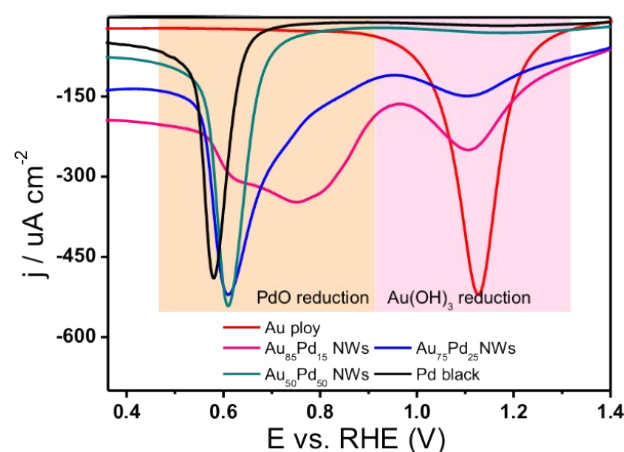


Figure S9. CV curves of Au polycrystalline electrode (AuPoly), Au-Pd nanowires with different Au/Pd ratios and Pd black in 0.5 M H₂SO₄ solution.

Table S1 Comparison of the H₂O₂ sensing performance in this work with that of other Au-Pd nanomaterials.

Sensing materials	Sensitivity (mM ⁻¹ cm ⁻²)	(μ A)Linear range	Detection limit	Ref.
Au NWs assembling spheres	6.25	up to 0.8 mM	1.2 μ M	[45]
Pd/PEDOT	215	2.5 μ M -1.0 mM	2.84 μ M	[48]
PdNP/AuNAE	533	up to 2 mM	5 μ M	[16]
AuPd nanocrystals	195.3	up to 3 mM	8.4 μ M	[47]
AuPd@GR	186.9	5 μ M -11.5 mM	1 μ M	[49]
Au-Pd/MoS ₂ /GCE	184.9	0.8 M - 10 mM	0.16 μ M	[50]
hAu ₁ Pd ₄ /GCE	5095.5	0.1-20 μ M	0.02 μ M	[51]
Au _{rich} Pd@AuPd _{rich} NWs	355	up to 10 mM	50 μ M	This work